Heating system performance estimation using optimization tool and BEMS data

Natasa Djuric[1*], Vojislav Novakovic[1], Frode Frydenlund[2]

1. Norwegian University of Science and Technology (NTNU),

Department of Energy and Process Technology, NO-7491 Trondheim, Norway

2. SINTEF Energy Research, NO-7465 Trondheim, Norway

[*]Corresponding author. E-mail address: natasa.djuric@ntnu.no. Address: Kolbjørn Hejes v. 1B, NO-7491, Trondheim, Norway. Phone: (+47) 73593338.

Abstract

Causes and effects of a few real faults in a hydronic heating system are explained in this paper. Since building energy management system (BEMS) has to be utilized in fault detection and diagnosis (FDD), practical explanations of faults and their related effects are important to building caretakers. A simple heat balance model is used in this study. The model is calibrated using the optimization tool. Site data from the BEMS of a real building are calibrated against the model. Desired and real data are compared, so that the effects of the following faults are analyzed: faults in an outdoor air temperature sensor, fault in the time schedule, and a water flow imbalance problem. This paper presents an overview of the real causes of the faults and their effects both on the energy consumption and the indoor air temperature. In addition, simple instructions for the building caretakers for fault detection in the hydronic heating systems are given.

Keywords: Hydronic heating; Optimization; Model calibration; Fault detection

1. Introduction

There has been much interest in the development of FDD techniques that are suitable for use in building control systems. There are many different diagnosis techniques and listed faults for the different HVAC systems [1]. A practical algorithm for diagnosing control loop problems of an air-handling unit (AHU) is provided in [2]. Deviations in the indoor temperature and energy consumption caused by different faults are explained practically, using an easy-to-use tool for FDD in [3]. Therefore, it is important to utilize more efficiently the FDD techniques and algorithms for the practical explanation of deviations in the indoor temperature and energy consumption. This study aims at the practical explanations of the operating faults in a hydronic heating system.

Most simulation models are based on first principles, such as *EnergyPlus*[1] [4]. A large number of parameters are needed as inputs for the simulation model. In addition, using optimization with *EnergyPlus* requires a whole lot of effort on pre-processing input files and post-processing results. While the work of S.W. Wang et al. [5]. shows that a kind of simplified models, which can represent the physical properties of the building system are preferred for diagnosis, optimal control etc. In addition, the 'grey box' approach, based on the laws of physics and a limited number of parameters, shows to be simple and flexible for the building performance estimation [6]. Therefore, this study uses the simplified heat balance model to describe the building and the hydronic heating system.

The calibration process compares the results of the simulation with measured data and tunes the simulation until its results closely match the measured data. A number of researchers have made progress in this topic [7]. Depending on the HVAC systems or

[1] Copyright by Lawrence Berkeley National Laboratories, Berkeley, CA, USA

building model, several different approaches for the model calibration have been found. The model calibration of the building stock that tunes the model to the average energy consumption involving a calibration coefficient, gives the low quality of validation data [8]. This study gives an approach for the calibration of the model on hourly basis using the optimization tool. There are often significant uncertainties associated with the definition of the models used to predict the performance. The nonlinearity in the HVAC system models makes the accurate model prediction difficult [9]. Therefore, sequential quadratic programming (SQP) [10] is necessary to use in this study. The successful use of SQP algorithm for the model calibration of a lumped simulation model is shown in [11]. The MATLAB optimization toolbox is used in this study to solve the optimization problem.

Effects of AHU sensor fault on total energy consumption are shown in the work of S.W. Wang et al. [12]. This paper gives the effects of two practical sensor faults in the hydronic heating system: a disconnected sensor and a faulty measurement of outdoor air temperature sensor. Two types of faults, an open window and a defective radiator valve, are studied by use of the model-based FDD in [13]. This paper gives few additional faults in the same system. Usually it is difficult to find the examples of real faults, so in the work of J.E. Pakanen et al. [14], a few artificial faults are introduced for on-line diagnostic tests of AHU. All the faults in our study are found on the case study building. Even though there have been lots of works in the building maintenance area, a combination of the optimization application and practical explanation in the hydronic heating system for these faults has not been reported.

The aim of this study is to utilize BEMS data, so that faults in a hydronic heating system can be detected. First the paper gives the building and the heating system

description. Afterwards a brief overview of the necessary data, including the explanation of the BEMS data and the additional measurements, is presented. Since the model is calibrated against the real data, the optimization application for the model calibration is explained. Based on the developed approach, the main part of the paper gives the effects of four found faults. Besides the two faults mentioned above, fault in the time schedule and a water flow imbalance problem are described.

Nomenclature

T	temperature $\left({}^{o}C\right)$
Q	energy consumption $\left(kWh\right)$
C_b	overall conductance of wall $\left(W/K\right)$
C_r	overall conductance of radiator $\left(W/K\right)$

Subscripts

out	outdoor
in	indoor
h	heating branch
t	hot tap water heating branch
v	ventilation
s	supply
r	return
i	time step
k	element index

2. Building description

This building description consists of: the general building data, the heating system description, a brief description of a heating system control strategy and a maintenance service structure for the BEMS.

The buildings are located at the University campus in Trondheim, Norway, and they consist of offices and laboratories. Two buildings have a common substation and they are connected. Therefore, they will be treated as one aggregate building in this study. The building has three floors and basement, and the total area is 13,700 m^2. Heat is supplied by district heating, indirectly connected to a heating network through the heat exchangers. The hydronic heating system has the central control provided by BEMS. Since the building is divided into four zones, there are four main branches in the substation. The building base with the orientation is shown in Figure 1. The schematic diagram of the hydronic system is given in Figure 2.

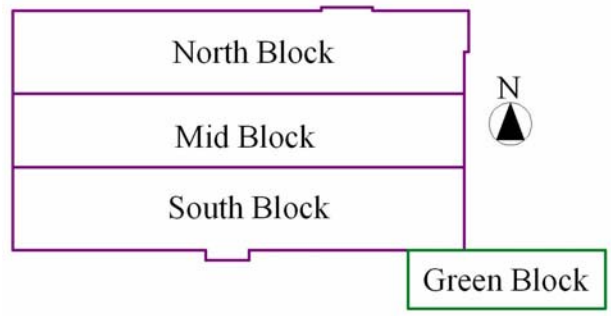

Figure 1. Sketch of the general building plan

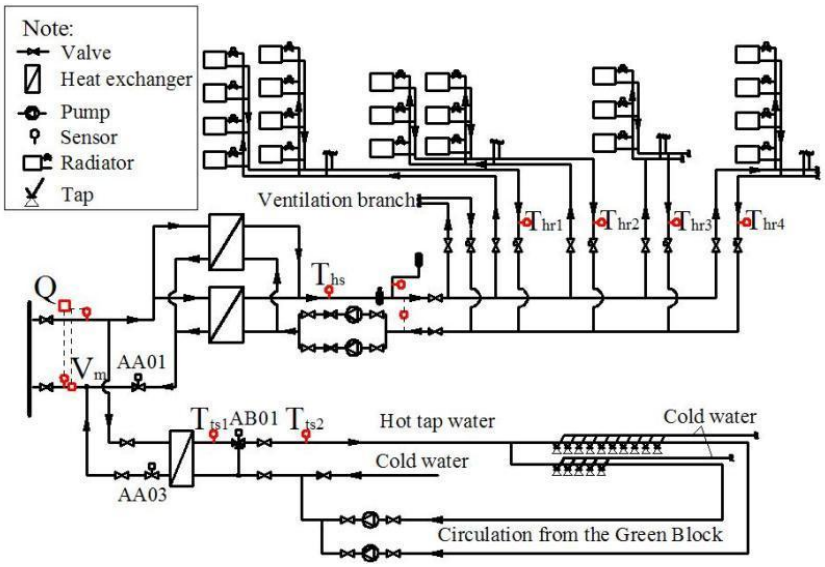

Figure 2. Schematic diagram of the hydronic system

Figure 2 shows the system with the measurement points that are logged in the BEMS. The Main Block, in Figure 2, consists of the North, the Mid and the South Block, all shown in Figure 1. The radiator heating system is controlled by the outdoor temperature compensation curve, which defines the supply-water temperature. The desired supply-water temperature is controlled by the sensor for the outdoor air temperature and the valve AA01 (Figure 2). The outdoor temperature compensation curve is given in Figure 3.

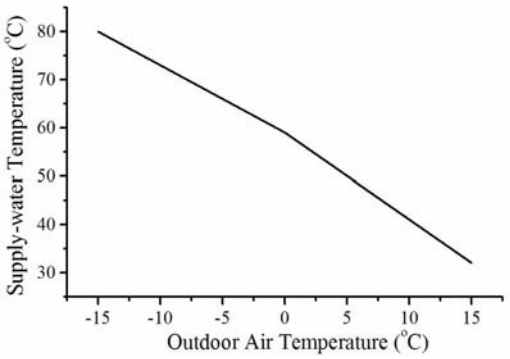

Figure 3. The outdoor temperature compensation curve

The supply-water temperature follows the curve from Figure 3 during the period 5 a.m. to 4 p.m., while during the period 4 p.m. to 5 a.m. this temperature is decreased by 10^oC. The same rule with the decreased supply-water temperature is implied during the weekends, except on Mondays, the rule from Figure 3 starts at 1 a.m. The desired indoor air temperature during working hours is 22^oC. The desired supply hot tap water temperature is 70^oC.

There are two levels of the maintenance service for the BEMS. The first level is provided by an internal maintenance personnel hired by the building maintenance service, and the second is provided by the BEMS supplier technical support.

3. Data collection and measurement

The aim of data collection was to get as many data as possible that can be used in the building performance estimation. In addition, these data should be used for a building model calibration, and for establishing a kind of rules for the faults detection. Data collecting includes: on-situ survey, data available from BEMS and additional measurements.

The on-situ survey was done by one person during one week. The radiators had been counted during the survey. These data are necessary for the model calibration.

The measurement adopted from BEMS includes the hourly log of the data. The additional measurement includes the following: the indoor air temperature in four offices, the outdoor air temperature, and the energy consumption of the hot tap water system by use of thermocouples and an ultrasound flow meter. In addition, the outdoor temperature is

downloaded from Norwegian Meteorological Institute [15]. Since the energy consumption for the hot tap water is not measured by the BEMS, it was necessary to measure it to establish the heat balance of the substation. The supply-water temperature is controlled by the outdoor air temperature sensor, so the sensor function test is useful for fault detection. Therefore the outdoor air temperature is measured and downloaded in addition to the BEMS data. All the other data are used both for the model calibration and the fault detection.

4. Model and model calibration

4.1. Model approach

The model approach in this study is based on the heat balance equations. The heat balance equations include: the zone heat balance and the heat balance for the substation. The ventilation systems are controlled locally, and they are all the simple fan coil units. There are two ways to define the energy consumption of the ventilation system: assuming an additional term in the heat balance equation or establishing the pressure balance model for the parallel branches (the four branches for heating and the branch for ventilation (Figure 2)). Since only the heat balance model is defined, only the total capacity of the ventilation is counted discretely as an additional term for each zone. The model is hourly based. Even though the model is steady-state, the building response is obtained by changing the temperature values.

The heat losses of the zones are described by C_b, the overall conductance of walls, which is a product of the heat conductance and the wall area. The heat capacity of the radiators is

calculated by use of overall conductance of radiator, C_r, and the mean temperature of the heating water based on [16]. The similar approach for defining the heat energy balance in such a system is applied in the work of M. Bojic et al. [17, 18]. The heat balance of a zone is shown in Figure 4.

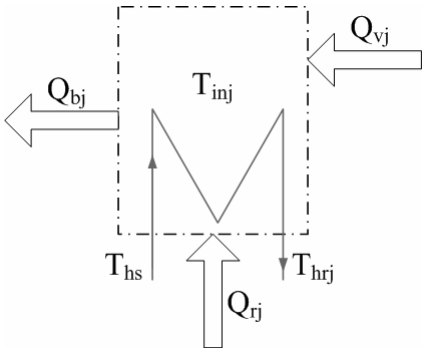

Figure 4. Heat balance of a zone

The dashed-doted line in Figure 4 bounds a zone. The heat balance for one zone can be written as:

$$Q_{bj,i} = Q_{rj,i} + Q_{vj,i} \tag{1}$$

where: $Q_{bj,i}$ is the hourly heat loss of a zone, $Q_{rj,i}$ is the heat capacity of the radiators in the zone *j*, and $Q_{vj,i}$ is the heat capacity of the ventilation system in zone *j*. Equation 1 can be written as:

$$C_{bj} \times \left(T_{inj,i} - T_{out,i}\right) = C_{rj} \times \left(\frac{T_{hs,i} + T_{hrj,i}}{2} - T_{inj,i}\right) + Q_{vj,i} \tag{2}$$

where: *j* is the zone index, and *i* is the time step. As Equation 2, the heat balance equations are established for each of the four zones. C_{bj}, C_{rj} and $Q_{vj,i}$ are the model parameters. Since there are four zones and *n* time steps, *4n+8* parameters are necessary to define the model.

After Equation 2 is solved, the hourly energy consumption of the radiators in each zone can be calculated as:

$$Q_{rj,i} = \frac{3600}{1000} \times C_{rj} \times \left(\frac{T_{hs,i} + T_{hrj,i}}{2} - T_{inj,i} \right). \quad (3)$$

The total hourly energy consumption of the building is:

$$Q = \sum_{j=1}^{4} Q_{rj,i} + \sum_{j=1}^{4} Q_{vj,i} + Q_{t,i} \quad (4)$$

where $Q_{t,i}$ is the energy consumption for the hot tap water that is measured.

The model input vector consists of the outdoor air and the supply-water temperature. The output vector contains *9n* elements, which are: the total energy consumption, the indoor air temperatures in each block, and the return-water temperatures from each block. Such a simple model is suitable for the optimization. Since this model will be calibrated against the real data, there is a necessity for simplifying the model and hence save simulation time, particularly in the optimization process as shown in the work of K.F. Fong et al [19].

4.2. Model calibration approach

The objective of the model calibration is to adjust the model to the related real data. In this case, the model calibration process calculates how close the model output corresponds to the measured data on an hourly basis. For every hour, a percentage difference, in paired data point, is calculated. The sum of squares percentage difference is then calculated for each hour. This sum allows for determination of how well the model fits to the data; the lower the sum, the better the calibration. The model is defined as:

$$Y_m = C \cdot X_m \tag{5}$$

where: Y_m is the vector of the model output, X_m is the vector of the model input, and C is the vector of the model parameters. The objective function for the calibration of the model in Equation 4 could be defined as

$$\min \sum_{k=1} \left(\frac{Y_{r,k} - Y_{m,k}}{Y_{r,k}} \right)^2 \tag{6}$$

where: $Y_{m,k}$ is the model output, and $Y_{r,k}$ is the corresponding measured data. To solve the optimization problem in Equation 6, it is necessary to use the SQP algorithm. The function 'LSQNONLIN' in the MATLAB optimization toolbox is employed to solve Equation 6 in this study.

In order to define an optimization problem, it is necessary to define the upper and lower bounds. The upper and lower bounds for the overall conductance of the radiator, C_r, in each block, are defined based on the on-situ survey. The upper and lower bounds for the overall conductance of the walls, C_b, are assumed based on the window size and U value. Considering the lack of information concerning the use of the ventilation systems, the lower and upper bounds for the ventilation capacities are chosen arbitrarily.

The $9n$ elements of the output vector are calibrated against the measured data using Equation 6. The output vector must have more elements than the model has parameters. In this case it means that $9n>4n+8$. An information flow for the model calibration is shown in Figure 5.

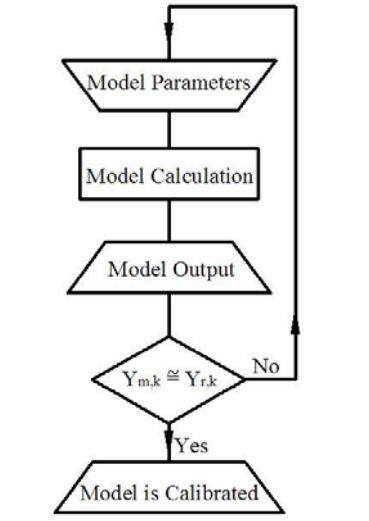

Figure 5. The information flow of the model calibration

Figure 5 shows that the optimization algorithm makes new model parameters input until the model outputs are adjusted to the corresponding measured data. The results of the model calibration are shown in Figure 6.

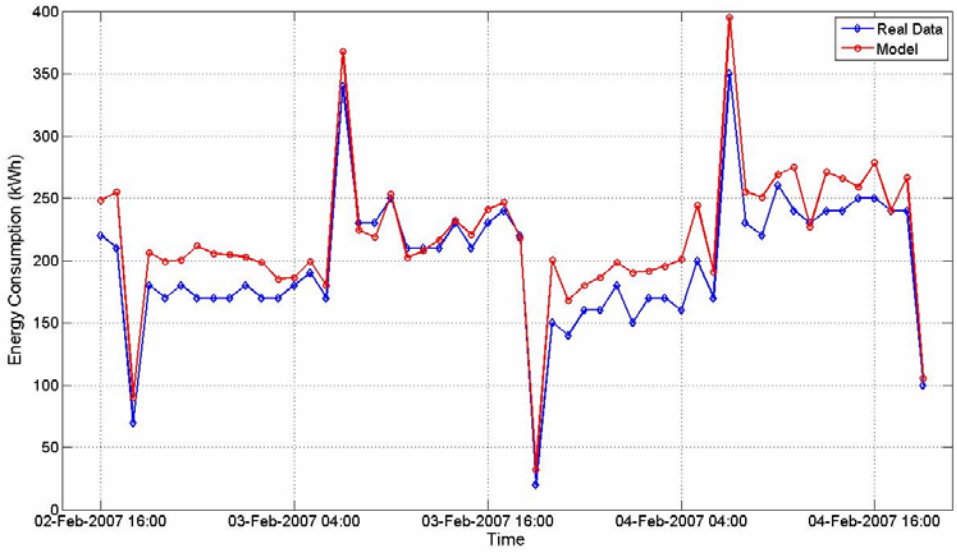

Figure 6. Results of the model calibration

Models are declared to be calibrated if they produces Mean Bias Error (MBE) within ±10% and Coefficient of Variation of the Root Mean Squared Error (CV(RMSE)) within ±30% when using hourly data [20]. The errors of the used model are given in Table 1.

Table 1. The error in the model outputs

	Q	T_{in1}	T_{in2}	T_{in3}	T_{in4}	T_{hr1}	T_{hr2}	T_{hr3}	T_{hr4}
MBE (%)	-9.82	-0.84	1.30	-1.87	-1.24	0.081	-0.13	0.20	-0.15
CV(RMSE) (%)	12.5	8.95	8.76	9.54	9.83	0.87	0.90	1.02	1.16

Table 1 shows that all the errors in the model outputs satisfy the condition from [20], so the model is calibrated.

The model is useable to estimate the changing both in the achieved indoor air temperature and energy consumption when there is a bias in the desired supply-water temperature. Since the existing energy management control strategies are mostly heuristic, there is a need for systematically examining and improving them, as mentioned in [21]. In this case, the supply-water temperature should always be tuned to obtain the desired indoor air temperature, so this model can be used to optimize it, too. A new outdoor temperature compensation curve can be found by minimizing the difference between the achieved and desired indoor air temperature. Such an optimization problem can be defined in a similar way as Equation 6, except that instead of the measured values, the desired values have to be used. Since the hot tap water consumption is measured and the model parameters for the ventilation are assumed, the model is not completely independent to predict the building performance. The model would be completely capable to predict when the model parameters are time independent. However, since the study includes both measurements

from BEMS and additional ones, there are data overlapping, so it is possible to analyze faults and their related effects on energy consumption and the indoor air temperature.

5. Faults in the heating system

Based on the developed approach, simple instruction for fault detection can be given. The following faults are noted: disconnected sensor for the outdoor air temperature, the outdoor air temperature sensor measures a faulty temperature, fault in the time scheduling program and a water flow imbalance problem in the substation. The faults are explained by first giving the cause and then the effects. The effects are shown on the total energy consumption and on the indoor air temperature of the Green Block. In the following figures the term “Desired Schedule” is used for the operation schedule described in connection with Figure 3. The term “Actual Schedule” appears in the following figures, and it implies the operation schedule actually in use. This schedule implies that the supply-water temperature follows the curve in Figure 3 from 5 a.m. to 5 p.m., Monday to Friday, and from 6 a.m. to 6 p.m., Saturday and Sunday. Outside of this period the supply-water temperature is decreased by $10^{o}C$.

5.1. Disconnected sensor

When the outdoor air temperature sensor is disconnected, the outdoor temperature compensation curve (Figure 3) is not fulfilled. The effects of such a fault are influenced by the BEMS strategy in the case when this sensor is disconnected.

The BEMS strategy for this heating system is defined so that if the sensor for the outdoor air temperature is disconnected, then the supply-water temperature is equal to the

corresponding value at $T_{out} = 0^{o}C$. Actually, the supply-water temperature would be almost constant regardless of the change in the outdoor temperature. Figure 7 shows the supply-water temperatures, the desired ones and the ones when the sensor is disconnected, normalized by the outdoor temperature.

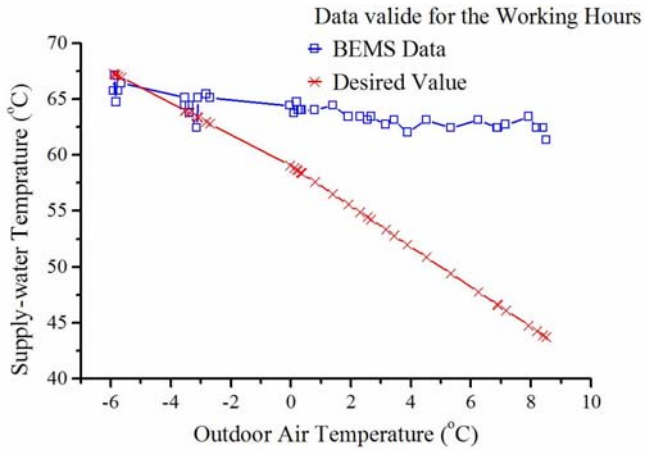

Figure 7. Supply-water temperature during Working Hours

Figure 7 shows the effect on the supply-water temperature when the outdoor air temperature sensor is disconnected during the working hours; the supply-water temperature is almost constant. The effect on the supply-water temperature during the off-working hours is the same as in Figure 7, except that all the values are approximately decreased by $10^{o}C$. In Figure 7 the faulty values of the supply-water temperature are higher than the corresponding value for the supply-water temperature at $T_{out} = 0^{o}C$ because there is also a water flow imbalance problem in the system.

Figure 8 shows the outdoor air temperature and the related supply-water temperatures, the measured and the desired.

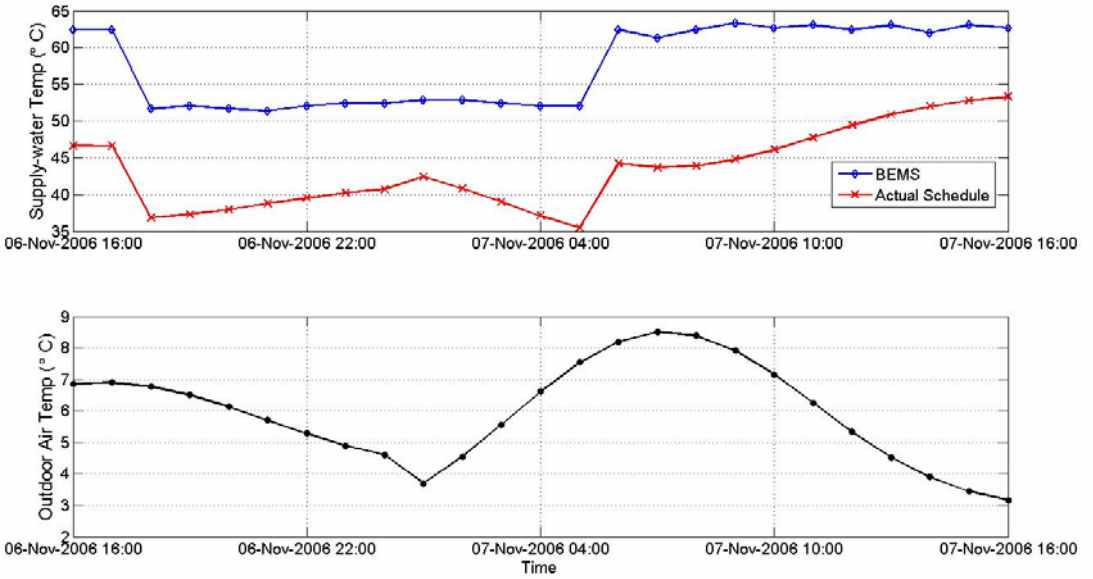

Figure 8. The disconnected sensor causes the constant supply-water temperature

The outdoor air temperature in Figure 8 is downloaded from the Norwegian Meteorological Institute [15]. The effects of the disconnected sensor for the same period are shown in Figure 9.

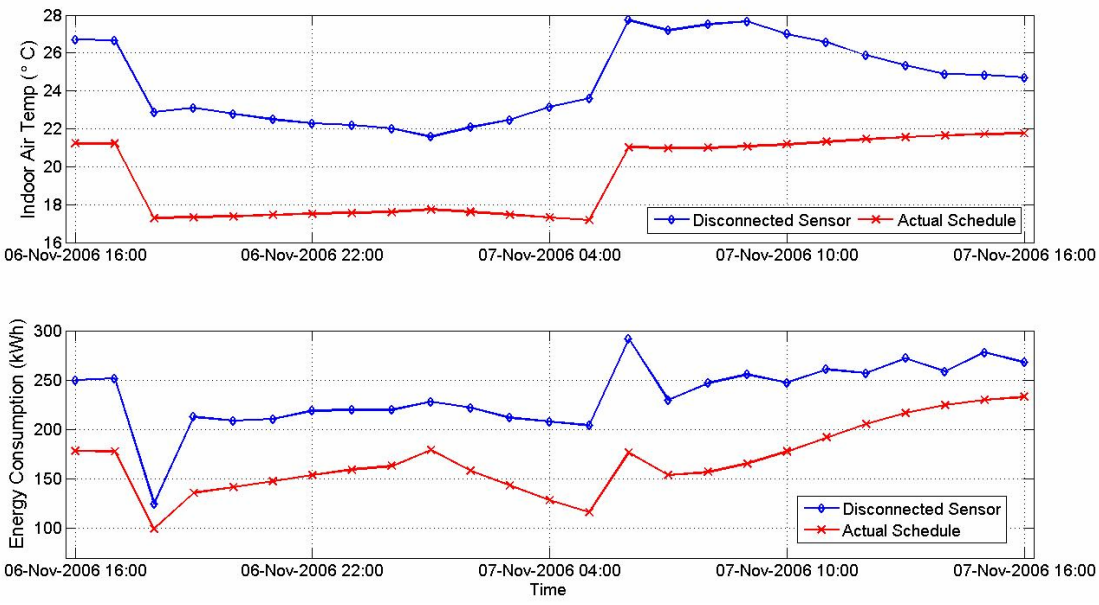

Figure 9. Effects on the indoor air temperature and the energy consumption when the outdoor air temperature sensor is disconnected

The effect of the disconnected outdoor air temperature sensor is shown in Figure 8, the supply-water temperature is almost constant regardless of the changes in the outdoor air temperature. When the outdoor air temperature sensor is disconnected, the indoor air temperature is different from the desired value, and the energy consumption is almost constant outside of the transient time period regardless of the outdoor air temperature changes, as Figure 9 shows. Since the current BEMS strategy in a case of the disconnected outdoor air temperature sensor is defined by the outdoor temperature of 0^oC, the supply-water temperature has the value close to an appropriate value at 0^oC. For a different BEMS strategy, this offset of the desired supply-water temperature is different. Actually, depending on the BEMS strategy the effects of the disconnected sensor are different. In this case, if $T_{out} > 0^oC$, then both the energy consumption and the indoor temperature are increased, while if $T_{out} < 0^oC$, both the energy consumption and the indoor temperature are decreased.

5.2. Fault in the outdoor air temperature sensor measurement

When the outdoor air temperature sensor measures faulty, the desired indoor temperature is not achieved even though the supply-water temperature seems to be achieved.

Since the outdoor temperature was obtained from three different sources, the sensor function test is possible to do by comparing these data as shown in Figure 10.

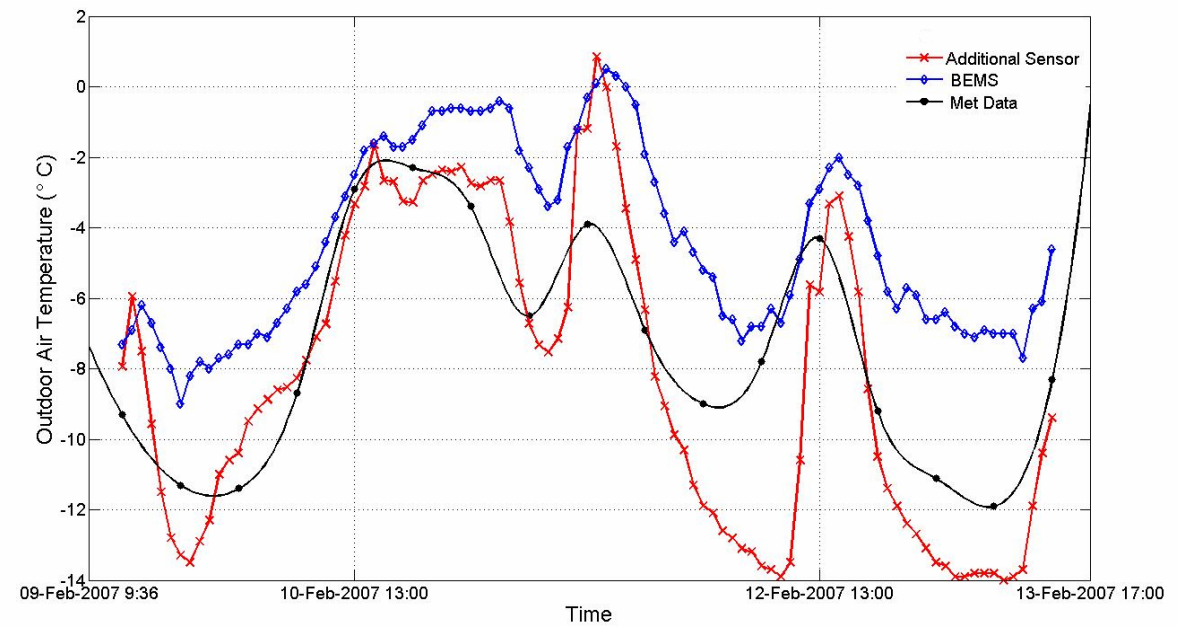

Figure 10. Different measurements of the outdoor air temperature

Figure 10 shows that the sensor used to control the supply-water temperature measures a faulty temperature. The line with crosses in Figure 10 represents the measurement done by an additional logger. This additional logger was placed outdoor all the time and logged the outdoor temperature every 10 minutes. The line named "Met Data" represents data from [15]. Since the Meteorological Institute gives data every six hours, these data are interpolated. In addition, the meteorological station is located at the different place from the actual building. In the further analysis the data for the outdoor air temperature measured by the additional logger are used as correct data.

If the outdoor air temperature sensor measures a faulty temperature, then the achieved supply-water temperature is faulty. In this case, the BEMS outdoor air temperature sensor measures a higher temperature than the actual one. Therefore, the supply-water temperature is lower than desired for the actual outdoor air temperature. The

difference between the outdoor air temperatures and related supply-water temperatures are shown in Figure 11.

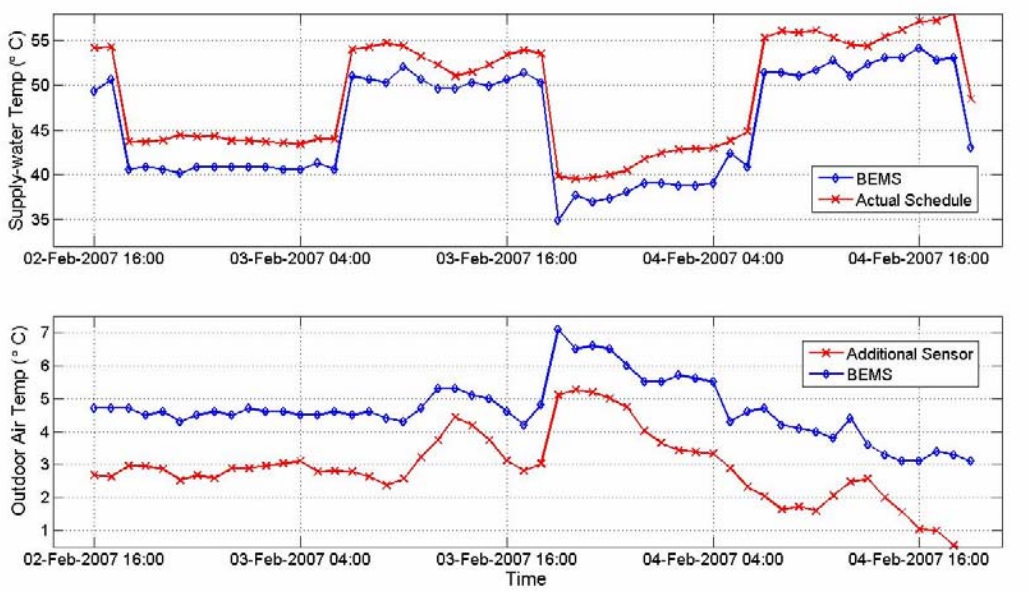

Figure 11. The BEMS outdoor air temperature sensor measures a faulty outdoor temperature

The example in Figure 11 shows the supply-water temperature when the outdoor sensor measures higher outdoor temperature than the actual one all the time. The corresponding effects of a fault in the outdoor air temperature sensor, both on the indoor air temperature and the energy consumption, are show in Figure 12.

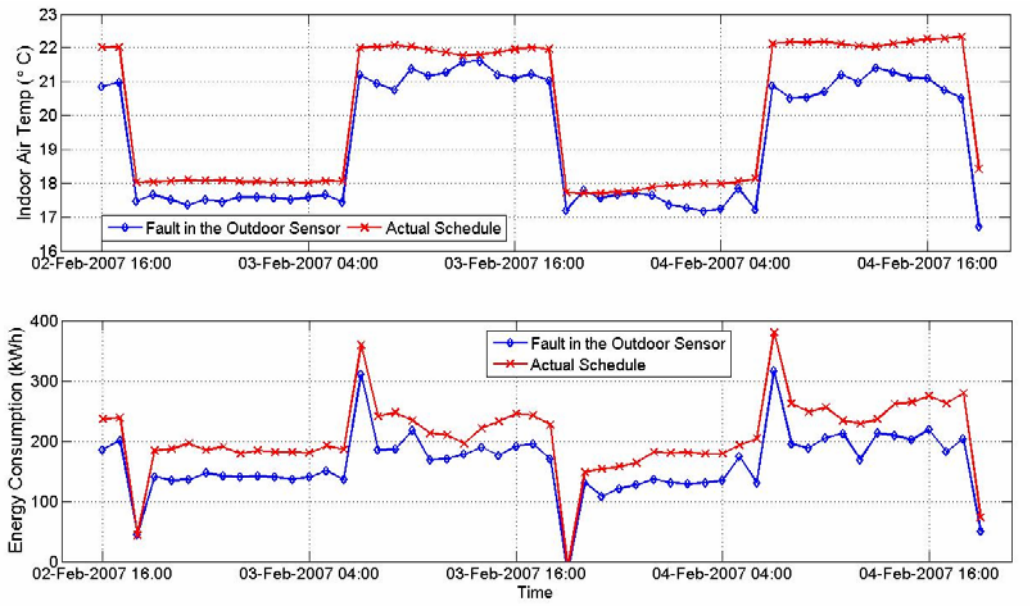

Figure 12. Effect of the faulty measurements of the outdoor air temperature sensor

Figure 11 shows that if the outdoor temperature sensor measures a higher temperature than the actual one, then the indoor temperature is decreased and the energy consumption is decreased. Such a fault can be noted by measuring the indoor temperature. If the indoor temperature is lower than desired, even though the supply-temperature achieves the desired value, then the outdoor sensor measures a wrong temperature. The cause of such a fault can be either a bad position of the sensor, an old sensor, or defected sensor by any reason.

5.3. Fault in time schedule

A fault in time schedule prevents an energy efficiency measure. Such a fault can be easily detected by checking the hourly energy consumption.

Since there are two maintenance levels that program the time schedule, it is possible that a fault appears. In connection with Figure 3, the desired operational schedule is given,

while the actual is given in the introduction of Chapter 5. The differences in the desired and actual operation schedule are shown in Figure 13. Since the real data are used in this example, the fault in the outdoor air temperature sensor measurement exists in Figure 13, as well.

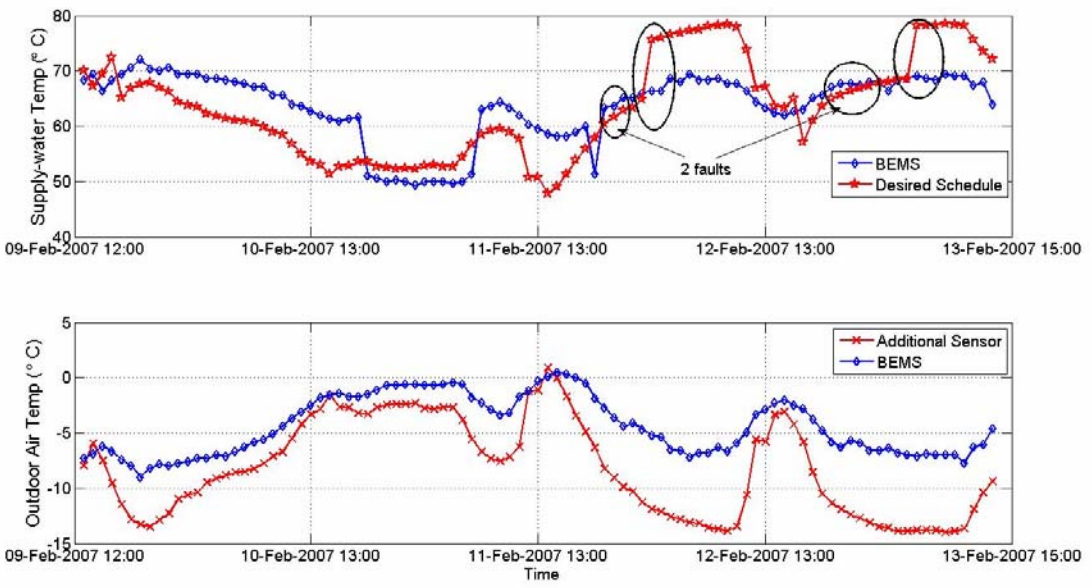

Figure 13. The different settings in the time schedule

Figure 13 shows that the desire schedule was not fulfilled. For example, February 9th to 11th was a weekend, i.e. the off-working hours, so according to the desired schedule the supply-water temperature should be $10^{o}C$ decreased. Since the actual schedule is in use, there is a difference in the achieved and desired supply-water temperature. In addition, Figure 13 shows that even though the outdoor air temperature sensor measures a faulty outdoor temperature, the achieved supply-water temperature is higher than desired, because the desired schedule is not in use. Figure 13 shows that the actual operational schedule is fulfilled only on February 10th, but at February 12th and 13th not at all. So in the off-working hours, between both February 11th and 12th, and 12th and 13th, the supply-water

temperature is the same as the desired, but this is because the actual schedule is not fulfilled (circles labeled with “2 faults” in Figure 13). The effects of this difference are shown in Figure 14.

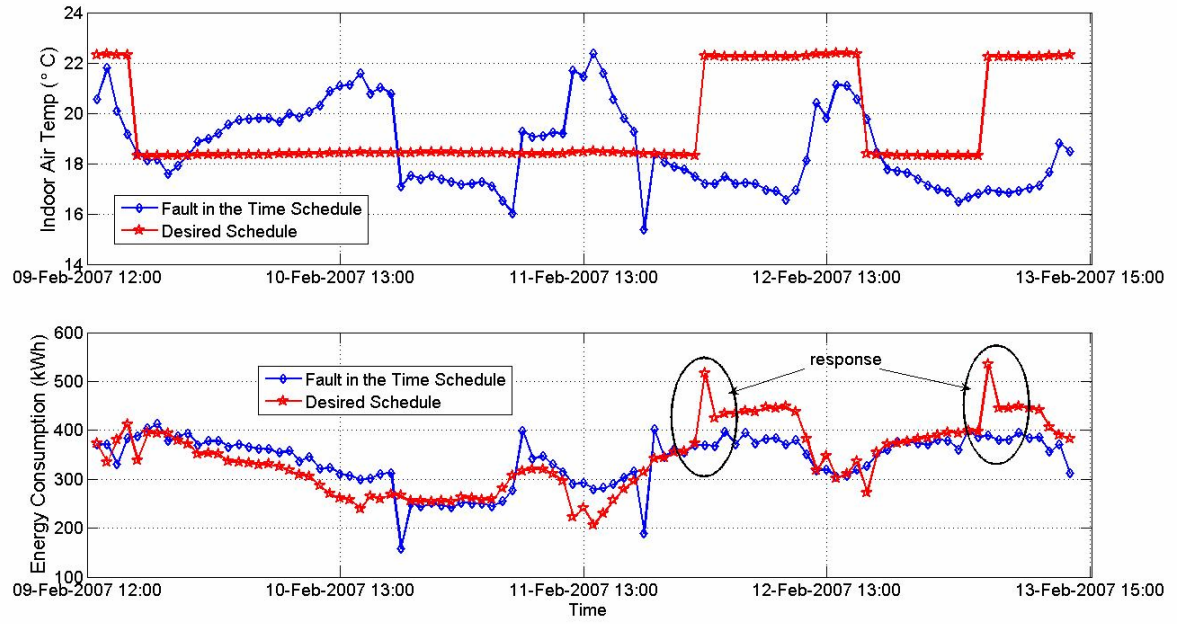

Figure 14. Effects of the different setting in the time schedule

Figure 14 shows the effects on the indoor air temperature and the energy consumption caused by the faults in the time schedule. Since the actual schedule was used during the weekend, the energy consumption is higher than it should be with the desired operation schedule. The desired operation schedule aims to be an energy efficiency measure. Since the actual schedule is in use, there is no effect of the energy efficiency measure. This difference in the time schedule can easily be noted by checking the hourly energy consumption. If there is no response in the hourly energy consumption at the moment the supply-water temperature is changed, it means that the desired time program is

not in use. The corresponding response in the energy consumption to the temperature changes in Figure 13 (labeled with ellipses) are labeled in Figure 14 (ellipses labeled with "response"). In addition to these different settings in the time schedule, it is possible that an error appears in the time schedule program, too. Such a fault can cause that the resulting operational schedule is neither actual nor desired, as it is shown for February 12th and 13th.

5.4. Water flow imbalance problem

This fault seems to be difficult to explain to the building caretakers. As a brief introduction into this fault a short example is given as follows: if the valve AA01 (Figure 2) does not close perfectly, the heating branch consumes energy, even though the BEMS data shows that the valve AA01 is closed. Therefore, the total energy consumption is increased.

The supply branches for the heating and the hot tap water system are parallel (Figure 2). A model for the hydraulic and thermal characteristics of these two branches is not defined in this study. Therefore, the effects cannot be shown as in the above examples, while the problem source is explained. These two branches have different hydraulic and thermal characteristics according to their purpose in the system. Since they are parallel, they influence each other, and a fault can appear. Such a fault is a fault made in the design phase. The example of such a fault is shown in Figure 15.

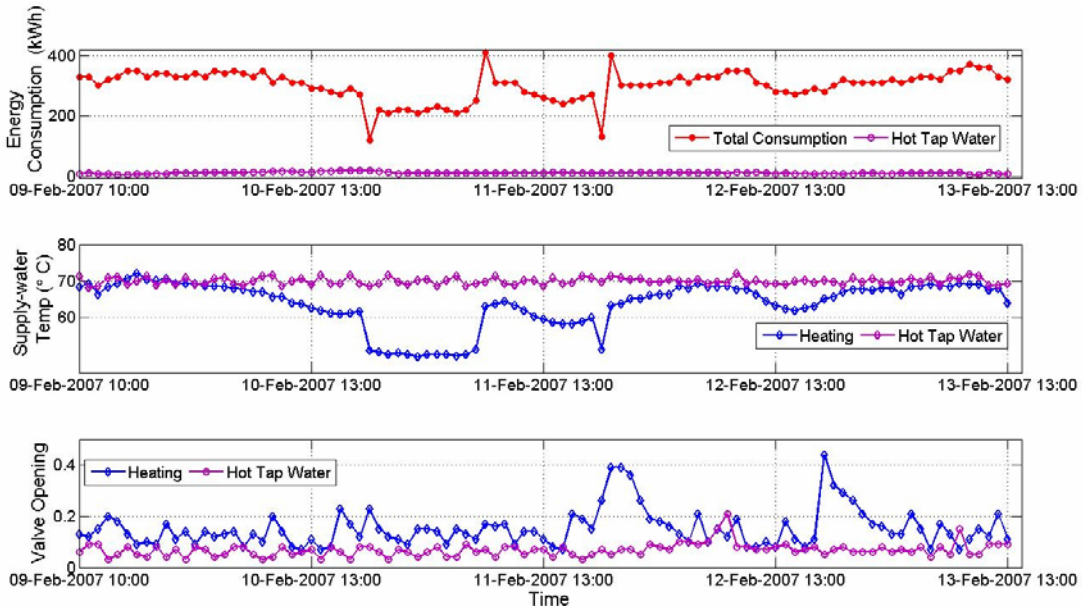

Figure 15. Problem between two parallel branches for the heating and hot tap water system

To present such a fault, the valve openings are also given in Figure 15. To explain this fault, it is necessary to look at the ratio between the hot tap water consumption and the total energy consumption. At the moment when the supply-water temperature is decreased by $10^{o}C$ this ratio is high. If the valve opening (AA01) for the heating system is increased at the same moment, the supply-water temperature for the hot tap water would be lower than the desired one, because the heating branch is capable of receiving a higher percentage of the total consumed energy. At the moment when the supply-water temperature is increased by $10^{o}C$, the total energy consumption is the highest, as at 6 a.m. February 11th. Since the entire system consumes a high amount of energy, the bias in the supply hot water temperature appears regardless of the valve position (AA03). Actually, when the supply-water temperature is almost constant for a period, the supply hot water temperature is influenced by the heating control valve (AA01) opening. The effect of this fault was noted

during the on-situ survey. A radiator at the first floor in the North Block was warm on July 4th 2006, when the outdoor air temperature was approximately $25^{o}C$. Even though the BEMS data showed that the valve AA01 opening was *0%*, it was possible that a certain amount of the main flow circulated through it, since the valve did not close perfectly. Since the consumption of the hot water was low, a part of the main flow circulated through the heating branch, so even the pump was shut down, the hot water circulated by itself. Therefore the total energy consumption is increased, even though nobody needs heating in the summer period.

6. Conclusion

The simple heat balance model of the building and the hydraulic heating system is calibrated against the real data by use of the optimization tool. The obtained model was good enough to detect four faults. Therefore the four detected faults in the hydronic heating system are explained. By use of the simple heat balance model the fault effects on the indoor air temperature and the energy consumption are shown. The results show that the faults can cause both increase and decrease in the achieved indoor air temperature and the energy consumption. The effects of the faults are influenced by when and how they appear.

The effects of the disconnected outdoor air temperature sensor are influenced by the BEMS strategy in the case of the disconnected outdoor air temperature sensor. The faulty measurement of the outdoor air temperature sensor influences the indoor temperature and energy consumption. The fault in the time schedule could appear because of both a few levels in the BEMS maintenance services and an error in the time schedule program. Such fault can be easily noted by checking the hourly energy consumption.

Further work should include the water pressure balance model, so that the model is completely independent of the additional measurements to predict the building performance by use of BEMS data. Currently and further detected faults and their effect should be summarized and classified, so that a kind of faults data base would be developed as a help to the building maintenance services.

Acknowledgements

This work is financially supported by the Research Council of Norway and the other members of the project: Life-Time Commissioning for Energy Efficient Operation of Buildings (project number 178450/s30).

References:

[1] J. Hyvarinen, S. Karki, Building Optimization and Fault Diagnosis Source Book, in IEA Annex 25, VTT, Finland, 1996.

[2] Salsbury T.I., A practical algorithm for diagnosing control loop problems, Energy and Buildings 29 (1999) 217–227.

[3] Young-Hak Song, Yasunori Akashi, Jurng-Jae Yee, A development of easy-to-use tool for fault detection and diagnosis in building air-conditioning systems, Energy and Buildings Article in press (2007)

[4] EnergyPlus, *EnergyPlus* Manual, 2006, Berkeley National Laboratory.

[5] S.W. Wang, X. Xinhua, Parameter estimation of internal thermal mass of building dynamic models using genetic algorithm, Energy Conversion and Management 47 (2006) 1927–1941.

[6] F. Deque, F. Ollivier, A. Poblador, Grey boxes used to represent buildings with a minimum number of geometric and thermal parameters, Energy and Buildings 31 (2000) 29–35.

[7] Y. Pan, Z. Huang, G. Wu, Calibrated building energy simulation and its application in a high-rise commercial building in Shanghai, Energy and Buildings Article in press (2006)

[8] Snakin J.-P.A., An engineering model for heating energy and emission assessment The case of North Karelia, Finland, Applied Energy 67 (2000) 353-381.

[9] X.F. Liu, A. Dexter, Fault-tolerant supervisory control of VAV air-conditioning systems, Energy and Buildings 33 (2001) 379-389.

[10] J. Nocedal, A. J. Wright, Numerical optimization, Springer series in operations research. 1999.

[11] C.-S. Park, G. Augenbroe, T. Messadi, M. Thitisawat, N. Sadegh, Calibration of a lumped simulation model for double-skin façade systems, Energy and Buildings 36 (2004) 1117–1130.

[12] S.W. Wang, F. Xiao, AHU sensor fault diagnosis using principal component analysis method, Energy and Buildings 36 (2004) 147–160.

[13] B. Yu, Ahc Van Paassen, S. Riahy, Open window and defective radiator valve detection, Building Service Engineering Research and Technology 24 (2003) 117–124.

[14] J.E. Pakanen, T. Sundquist, Automation-assisted fault detection of an air-handling unit; implementing the method in a real building, Energy and Buildings 35 (2003) 193–202.

[15] Norwegian Meteorological Institute. [cited; Available from: http://met.no/index.shtml.

[16] Todorovic Branislav, Designing the plants for central heating, 2000, Belgrade: Faculty of Mechanical Engineering, Belgrade.

[17] M. Bojic, N. Trifunovic, S.I. Gustafsson, Mixed 0–1 sequential linear programming optimization of heat distribution in a district-heating system, Energy and Buildings 32 (2000) 309–317.

[18] M. Bojic, N. Trifunovic, Linear programming optimization of heat distribution in a district-heating system by valve adjustments and substation retrofit, Building and Environment 35 (2000) 151-159.

[19] K.F. Fong, V.I. Hanby, T.T. Chow, HVAC system optimization for energy management by evolutionary programming, Energy and Buildings 38 (2006) 220–231.

[20] Measurement of Energy and Demand Savings, Vol. Guideline 14 2002: ASHRAE.

[21] W.Z. Haung, M. Zaheeruddin, S.H. Cho, Dynamic simulation of energy management control functions for HVAC systems in building, Energy Conversion and Management 47 (2006) 926–943.